CONF-951128--4
BNL-62219

A PLANE STRAIN MODEL OF SOIL SATURATION EFFECT ON DYNAMIC STIFFNESS FUNCTIONS OF EMBEDDED FOOTINGS*

by

Nikolaos Simos, A.J. Philippacopoulos and M. Reich
Brookhaven National Laboratory
Upton, NY 11973

Thomas McSpadden
U.S. Department of Energy
Washington, DC 20585

ABSTRACT

Impedance functions associated with horizontal and vertical vibrations of rigid massless strip footings embedded in a saturated soil stratum are evaluated using a finite element approach. The foundation medium is treated as a two-phase continuum which behaves according to Biot's classical theory of wave propagation in fluid-saturated porous media. Parametric studies have been recently performed by the authors in an effort to verify that the adopted finite element approach and associated numerical procedures yield reasonable correlations with analytic solutions of soil-structure interaction problems.

Horizontal and vertical impedance functions are presented for various *embedment depth/soil layer thickness* configurations. It is shown that saturation influences the foundation impedances especially their imaginary parts which can be reasonably explained as being the result of additional dissipation in the system associated with the motion of pore fluid relative to the soil skeleton. It is further shown that, as anticipated, soil stiffnesses increase with increasing embedment depth.

INTRODUCTION

Dynamic response of foundations interacting with saturated media has drawn a lot of attention primarily because of the effect of pore fluid on response. This study focuses on such effects as they are related to foundation impedances. Specifically, the system treated involves rigid foundations embedded in saturated strata. The case of a strip footing is analyzed.

The approach used is based on finite element modeling taking into account the two-phase nature of the underlying medium. Solution procedures were implemented into the computer code POROSLAM [1] the formulation of which is based on a discretization of Biot's 2-D coupled equations of motion under plane strain conditions. Both the solid and the fluid displacements are discretized in the near field while the far field is simulated with transmitting boundaries. Such formulation is consistent with acceptable techniques used to simulate infinite media for dry foundation conditions. The additional factor is the inclusion of the fluid motion and pore pressure field associated with the saturated medium.

Impedance functions for such media, but limited to surface type foundations, have been obtained in previous studies with POROSLAM in [1], [2], [3]. Similarly, impedance functions of footings embedded in saturated strata were obtained in [4]. These studies are extended here to include both horizontal as well as vertical impedances of embedded strip footings which could be of

*This work was performed under the auspices of the U.S. Department of Energy.

significant interest in engineering applications of soil-structure interaction to seismic problems.

In the following two sections the theoretical model in the form of the coupled equations of motion with appropriate boundary conditions as well as the finite element representation of the problem are presented. Results with the finite element method are expected to be as good as the theory it is formulated upon with deviations that stem from the discretization of the 2-D system. In previous studies [4], the effectiveness of the method in treating the dynamic response of strip footings was addressed by comparing the finite element results with analytic solutions. Specifically, a series of numerical evaluations were made with POROSLAM [4] for surface foundations resting on dry half spaces and the results were compared with corresponding analytical solutions obtained by Luco *et al* [5]. In addition, 1-D analytic solutions for wave propagation problems in saturated media were compared with corresponding solutions for discrete models yielded by POROSLAM. Comparisons of the finite element results with the analytical solutions are listed in [4] and demonstrate that POROSLAM solutions show good agreement for both problems of interest.

This paper presents a series of solutions for the horizontal and vertical impedance functions of footings embedded in saturated media. Of particular interest reflected in the type of problems analyzed, is the effect of variations between the width of the footing, the depth of the embedment and of the stratum thickness. The influence of certain properties of the underlying saturated medium on the foundation impedances is addressed in [6]. In that study, parametric variations are presented in terms of soil permeability, dissipation in the matrix material, porosity, etc.

The main trend observed in the results obtained in this study, is a relative increase in the imaginary part of the impedance functions. This is attributed to the additional damping caused by the relative motion of the pore fluid through the soil skeleton. It is also shown that soil stiffness increases with increasing embedment depth in the lower half of the frequency range. This may be attributed to the role of the pore pressure at the footing/soil interface.

PROBLEM STATEMENT

The system analyzed is shown in Figure 1. The foundation has width **2b**, embedment depth **D** and is considered to be massless, rigid and impervious. The stratum has depth **H** and it is saturated up to the surface (y = 0).

With respect to the cartesian coordinate system x - y and under plane strain conditions:

$[u_x, u_y]$	=	solid displacements
$[w_x, w_y]$	=	fluid displacements
$[\sigma_{xx}, \sigma_{yy}, \sigma_{xy}]$	=	intergrannular stresses
p_f	=	pore fluid pressure

The total stress vector is:

$$\{\tau\} = \{\sigma_{xx} - \alpha p_f,\ \sigma_{yy} - \alpha p_f,\ \sigma_{xy}\}^T \quad \textbf{(1)}$$

The governing equations of motion are:

$$\frac{\partial \tau_{xx}}{\partial x} + \frac{\partial \tau_{xy}}{\partial y} = \varrho \ddot{u}_x + \varrho_f \ddot{w}_x \quad \textbf{(2a)}$$

$$\frac{\partial \tau_{yx}}{\partial x} + \frac{\partial \tau_{yy}}{\partial y} = \varrho \ddot{u}_y + \varrho_f \ddot{w}_y \quad \textbf{(2b)}$$

and

$$-\frac{\partial p_f}{\partial x} = \varrho_f \ddot{u}_x + \frac{1}{f}\varrho_f \ddot{w}_x + \frac{\eta}{k}\dot{w}_x \quad \textbf{(2c)}$$

$$-\frac{\partial p_f}{\partial y} = \varrho_f \ddot{u}_y + \frac{1}{f}\varrho_f \ddot{w}_y + \frac{\eta}{k}\dot{w}_y \quad \textbf{(2d)}$$

where,

f = porosity, ϱ = total mass density, ϱ_f = fluid mass density, α = compressibility of solid, M = compressibility of pore fluid, η = fluid viscosity, and k = soil permeability.

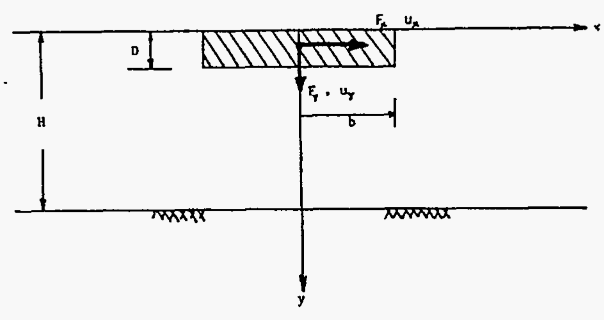

Figure 1. Problem Description

DISCLAIMER

Boundary Conditions

Constraint conditions associated with the vanishing of stresses at the free surface, continuity of stresses and displacements along the far boundaries and interface conditions between the footing and the surrounding soil are imposed as follows:

At the free-Surface ($y = 0$ & $|x| > b$):

$$\sigma_{yy} = \tau_{xy} = p_f = 0 \tag{3a}$$

At the footing/stratum interface:

(a) Vertical motion

$$u_y = \Delta_y e^{i\omega t} \quad u_x = 0 \tag{3b}$$

(b) Horizontal motion

$$u_x = \Delta_x e^{i\omega t} \quad u_y = 0 \tag{3c}$$

while for both cases,

$$|x| \leq b \text{ and } y = D: \quad w_y = 0 \tag{3d}$$

and

$$|x| = b \text{ and } 0 \leq y \leq D: \quad w_x = 0 \tag{3e}$$

At the bottom of soil layer ($y = H$)

$$u_x = u_y = w_y = 0 \tag{3f}$$

FE IMPLEMENTATION

The discretized form of the coupled equations (2) in the finite element formulation is expressed as

$$\{\tau\} = E_c\left([D_1]\left\{[D_1] + [D_3]\frac{\vartheta}{\vartheta t}\right\}\right)\{u_x, u_y\}^T + \alpha^2 M[D_2]\{u_x, u_y\}^T + \alpha M[D_2]\{w_x, w_y\}^T \tag{4a}$$

where,

$$[D_0] = \begin{bmatrix} 1 & \dfrac{\nu}{1-\nu} & 0 \\ \dfrac{\nu}{1-\nu} & 1 & 0 \\ 0 & 0 & \dfrac{1-2\nu}{2(1-\nu)} \end{bmatrix} \tag{4b}$$

$$[D_3] = \begin{bmatrix} \xi_c & \dfrac{\xi_c \nu}{1-\nu} & 0 \\ \dfrac{\xi_c \nu}{1-\nu} & \xi_c & 0 \\ 0 & 0 & \dfrac{\xi_s(1-2\nu)}{2(1-\nu)} \end{bmatrix} \tag{4c}$$

$$[D_1] = \begin{bmatrix} \dfrac{\vartheta}{\vartheta x} & 0 \\ 0 & \dfrac{\vartheta}{\vartheta y} \\ \dfrac{\vartheta}{\vartheta y} & \dfrac{\vartheta}{\vartheta x} \end{bmatrix} \quad [D_2] = \begin{bmatrix} \dfrac{\vartheta}{\vartheta x} & \dfrac{\vartheta}{\vartheta y} \\ \dfrac{\vartheta}{\vartheta x} & \dfrac{\vartheta}{\vartheta y} \\ 0 & 0 \end{bmatrix} \tag{4d}$$

and

$$p_f = -\alpha M(e_{xx} + e_{yy}) - M\left(\frac{\vartheta w_x}{\vartheta x} + \frac{\vartheta w_y}{\vartheta y}\right) \tag{4e}$$

ξ_c is the hysteretic damping ratio associated with dilatational deformation while ξ_s represents the damping ratio associated with shear deformation. E_c is given by:

$$E_c = \frac{(1-\nu)E}{(1+\nu)(1-2\nu)} \tag{4f}$$

Finite element analysis of the problem is subject to the following computational aspects:

a. Simulation of radiating conditions at the sides of the finite element mesh using transmitting boundaries. Similarly, when half-space solutions are sought, then the bottom boundary is also modeled with transmitting boundaries.

b. A fineness of mesh that will allow transmission of the frequencies used for the computation of impedance functions. Typically, element sizes of 1/6 of the wavelength were used. The dimensionless frequencies studied were up to $\alpha_{max} = 5.0$.

c. A fineness of mesh along the interface between the footing and the surrounding medium such that reasonable estimates of the resultant forces associated with the impedance functions are obtained.

$$F_i = \int_c \tau_{ij}\, ds \quad ; \quad i,j = x,y$$

c = footing/medium interface

τ_{ij} = bulk stress defined in equation 1.

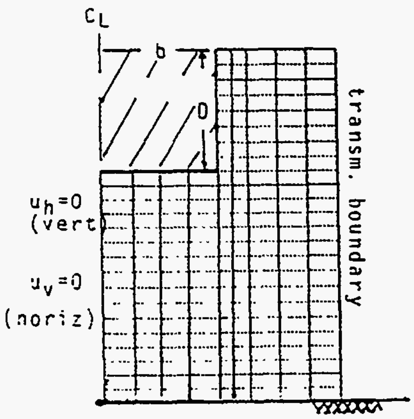

Figure 2. Finite Element Representation

Figure 2 depicts the finite element discretization of the soil stratum along with the imposed continuity and constraint conditions. Half of the domain is discretized and thus symmetry conditions are imposed along the axis x = 0. Specifically, for the vertical motion of the footing

$$x = 0 \text{ and } y > D : \; u_x = w_x = 0 \qquad \textbf{(5a)}$$

while for horizontal motion,

$$x = 0 \text{ and } y > D : \; u_y = w_y = 0 \qquad \textbf{(5b)}$$

IMPEDANCE FUNCTIONS

The equations of motion of the system expressed through equations (2) and (4), along with the specified boundary conditions (3) and (5), are solved numerically with the POROSLAM computer code. To ensure that the computational analysis indeed captures the dynamic response of the footing, several benchmark analyses have been performed [4]. Specifically, a set of 1-D wave propagation problems in saturated media were analyzed with POROSLAM and then compared with corresponding analytic solutions. Results for the soil and pore fluid displacement amplitudes as well as amplitudes of pore pressure and intergranular stresses are given in [4]. The agreement between the two approaches is excellent. To further validate the ability of the code to analyze footing vibration problems, comparisons of horizontal and vertical compliances were made with available analytical solutions [5]. Comparative results given in [4] show good agreement with, as expected, some differences in the very low frequency range where analytical solutions become singular. The above verification benchmark problems provided reasonable confidence in the ability of the POROSLAM computer code to compute the dynamic response of foundations.

Horizontal and vertical impedances of rigid strip footings embedded on saturated strata were evaluated based on two geometrical ratios which are expected to influence the results. These are:

a. the ratio of the embedment (or footing) half-width (b) to the embedment depth (b/D),

b. the ratio of the stratum thickness (H) to the embedment half-width (H/b).

Four different FE models were analyzed, each of them, for both horizontal and vertical motions.

The soil stratum properties were assumed to remain constant throughout the analysis. The effect of soil parameter variation is addressed in a different study [6]. Hysteretic damping ξ was taken as 5% and the Poisson's ratio as $\nu = 1/3$. In addition, the porosity of the stratum was taken as 30%, the permeability as 0.001 ft/sec and the viscosity was selected such that $\frac{\eta}{k} = 1000 \, \frac{lbf\text{-}\sec}{ft}$. The pore fluid is treated as incompressible. Impedances were computed up to the dimensionless frequency $\alpha_0 = \frac{\omega b}{V_s} = 5.0$. Impedance functions were expressed in the form,

$$K_{vv} = k_{vv} + i\alpha_0 c_{vv} \qquad \textbf{(6a)}$$

$$K_{hh} = k_{hh} + i\alpha_0 c_{hh} \qquad \textbf{(6b)}$$

where k_{vv} and k_{hh} are the real parts of the impedance functions while c_{vv} and c_{hh} are their imaginary counterparts.

Figures 3, 4 and 5 depict the variation of the vertical impedance functions with frequency, for geometric ratios H/R= 2, H/R = 3 and H/R = ∞ (half space) respectively. Each figure displays the real and the associated imaginary part for width to embedment depth ratios R/D = 1 and R / D = 2. Vertical impedance functions for the corresponding dry cases are shown in Figures 6, 7 and 8. The latter cases were analyzed in order to assess the influence of the pore fluid on the impedances for identical geometric configurations.

Horizontal impedance functions under saturated condition of the soil are presented in Figures 9, 10 and 11 while the corresponding dry cases for the horizontal impedances are shown in Figures 12, 13 and 14, respectively.

CONCLUSIONS

Horizontal and vertical impedance functions for rigid, massless foundations embedded in a fluid-saturated poroviscoelastic stratum have been obtained utilizing the POROSLAM computer code. Results for both saturated and dry foundation conditions were developed for direct comparison and assessment. The effect of the embedment depth as well as of the thickness of the underlying soil layer were sought in the evaluated cases. From the results obtained it appears that the presence of the pore fluid influences the dynamic interaction between the foundation and the soil. Specifically, in the vertical case there is a relative increase in the imaginary part of the impedance attributed to the additional damping resulting from the motion of the pore fluid relative to the solid matrix material. Further, for this case, the stiffness part in the low frequencies was not affected much by the pore fluid presence. Pore fluid effects become apparent at higher frequencies where they are accompanied by differences in system frequencies which in turn signify differences in wave speeds between the saturated and the corresponding dry media. Similar conclusions were drawn for the dissipation part of the horizontal case (more dissipation in the lower frequency range when the pore fluid is present and a shifting of the system frequencies). The stiffness part of the horizontal impedances is unaffected by saturation in the very low frequency range (almost static) but exhibits an increase in the mid-frequency range. It is further observed that, besides the frequency shift, the amplitude differences between the dry and the saturated cases are far less pronounced than those observed in the vertical case. It should also be noted that, as anticipated, there is an increase in the stiffness part of the impedance with increasing embedment depth.

In general, based on the results of the analysis, the observed influence of the pore fluid is not of primary significance for typical soil-structure interaction applications. The importance of this analysis, however, is in capturing the soil stress and pore pressure fields in the vicinity of the foundation/stratum interface. Potential soil liquefaction during the process of dynamic interaction could significantly affect the response of the foundation.

REFERENCES

1. N. Simos, C.J. Costantino and C. Miller, *POROSLAM. Two-Dimensional Dynamic Solution of Elastic Saturated Porous Media*, Earthquake Research Center, City University of New York, 1988.

2. N. Simos, M. Reich, *Seismic Analysis of the PAR POND DAM, Study of Slope Failure and Liquefaction*, Technical Report BNL-52450, 1994.

3. C.J. Costantino and A.J. Philippacopoulos, *Influence of Ground Water on Soil-Structure Interaction*, NUREG/CR-4784, 1987.

4. A.J. Philippacopoulos, N. Simos and T. McSpadden, *Impedance Functions of Footings Embedded in Saturated Strata*, Proceedings of the 27th Joint Meeting of US-JAPAN Panel on Wind and Seismic Effects, May 1995.

5. J.E. Luco, R.A. Westmann, *Dynamic Response of a Rigid Footing Bonded to an Elastic Half Space*, Journal of Applied Mechanics, Paper No. 71-APMW-15, 1972.

6. A.J. Philippacopoulos and N. Simos, *A Parametric Study of Dynamic Response of Strip Foundation on Saturated Media*, Proceedings of 32nd SES, (to appear).

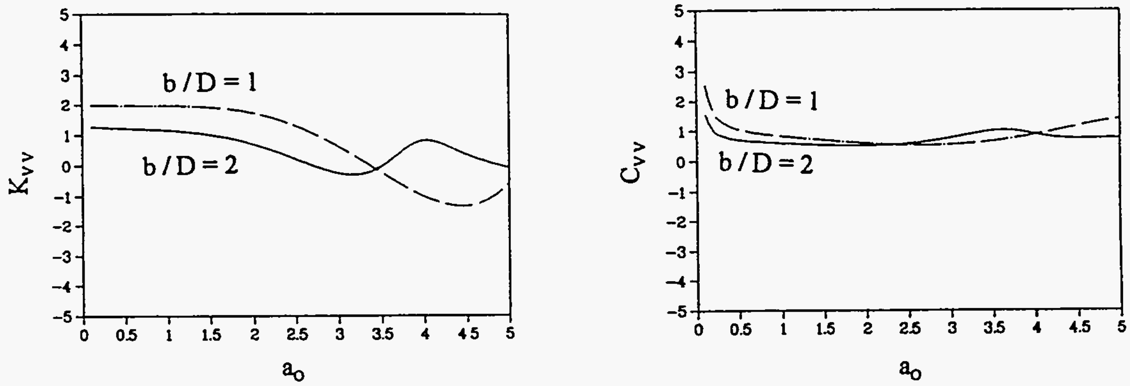

Figure 3. Vertical Impedances. Case: H/b = 2 Saturated Stratum ($\nu = \frac{1}{3}\,; \xi = 0.05$)

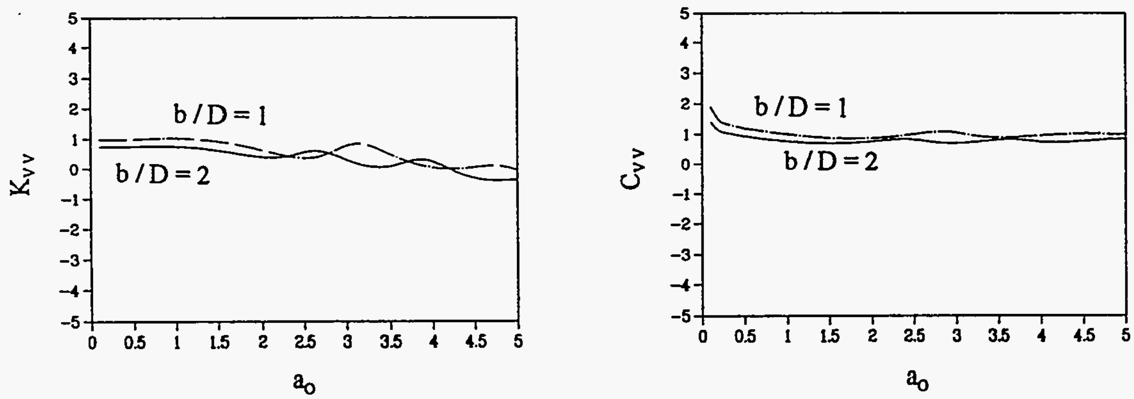

Figure 4. Vertical Impedances. Case: H/b = 3 Saturated Stratum ($\nu = \frac{1}{3}\,; \xi = 0.05$)

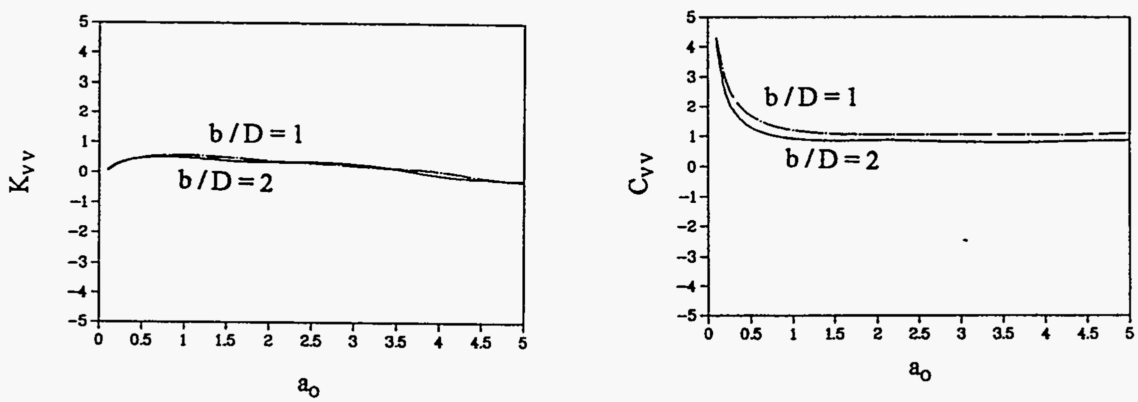

Figure 5. Vertical Impedances. Case: H/b = ∞ Saturated Stratum ($\nu = \frac{1}{3}\,; \xi = 0.05$)

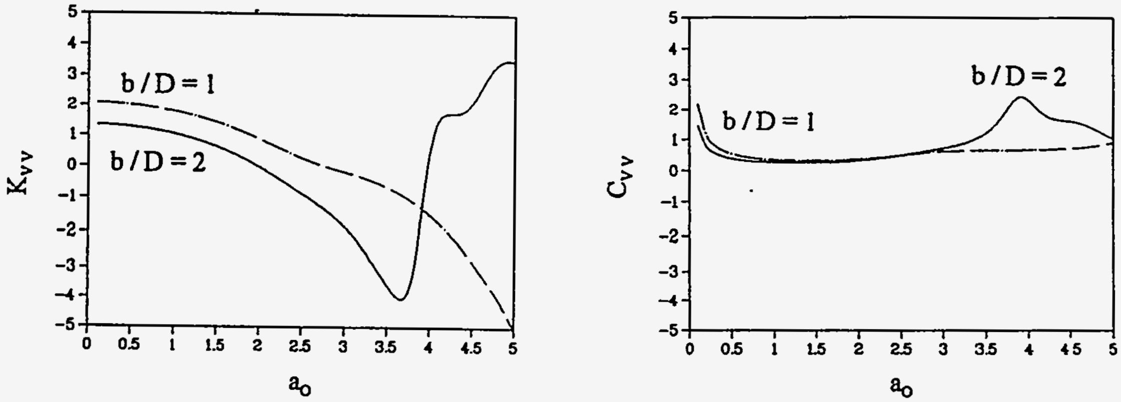

Figure 6. Vertical Impedances. Case: H/b = 2 Dry Stratum ($\nu = \frac{1}{3}$; $\xi = 0.05$)

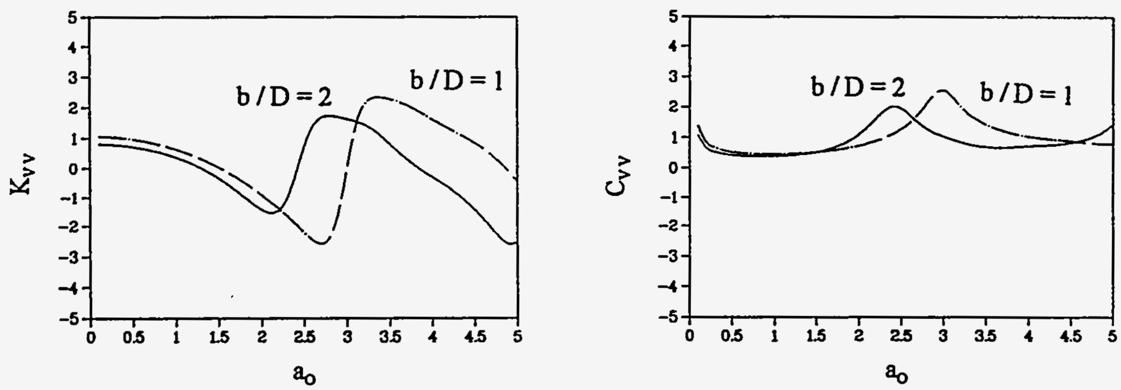

Figure 7. Vertical Impedances. Case: H/b = 3 Dry Stratum ($\nu = \frac{1}{3}$; $\xi = 0.05$)

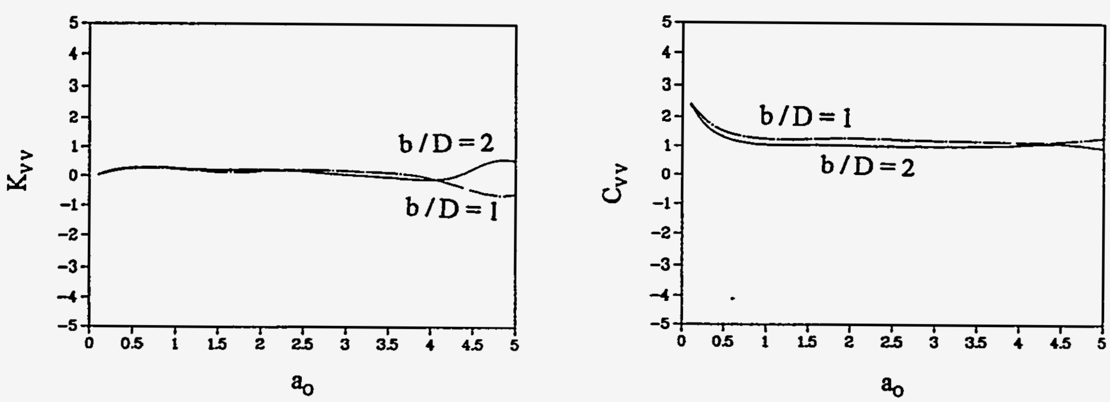

Figure 8. Vertical Impedances. Case: H/b = ∞ Dry Stratum ($\nu = \frac{1}{3}$; $\xi = 0.05$)

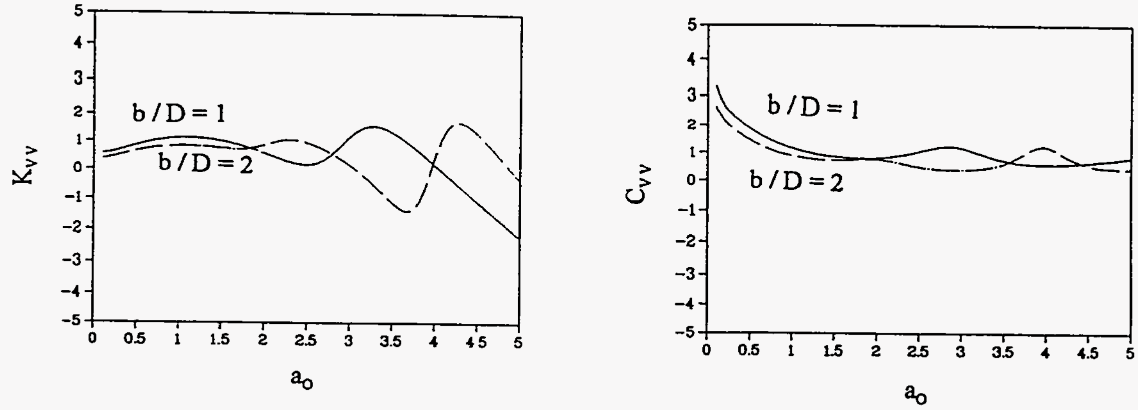

Figure 9. Horizontal Impedances. Case: H/b = 2 Saturated Stratum ($\nu = \frac{1}{3}$; $\xi = 0.05$)

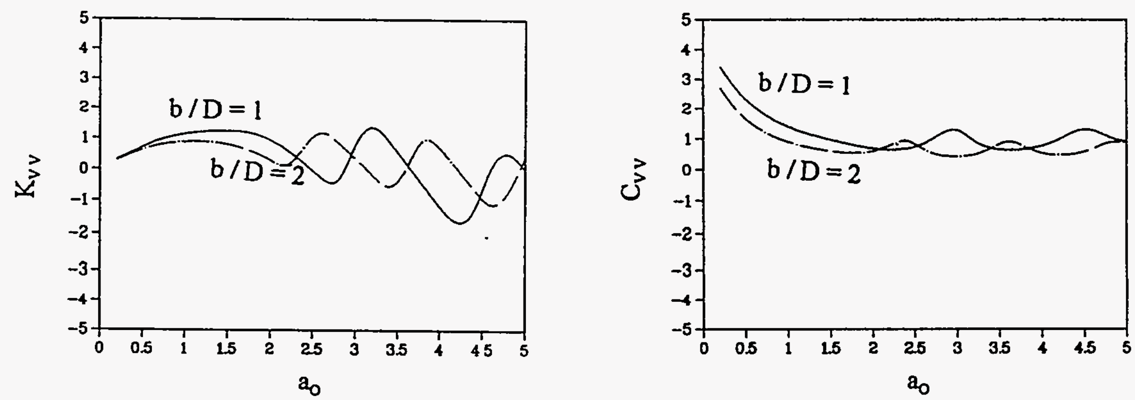

Figure 10. Horizontal Impedances. Case: H/b = 3 Saturated Stratum ($\nu = \frac{1}{3}$; $\xi = 0.05$)

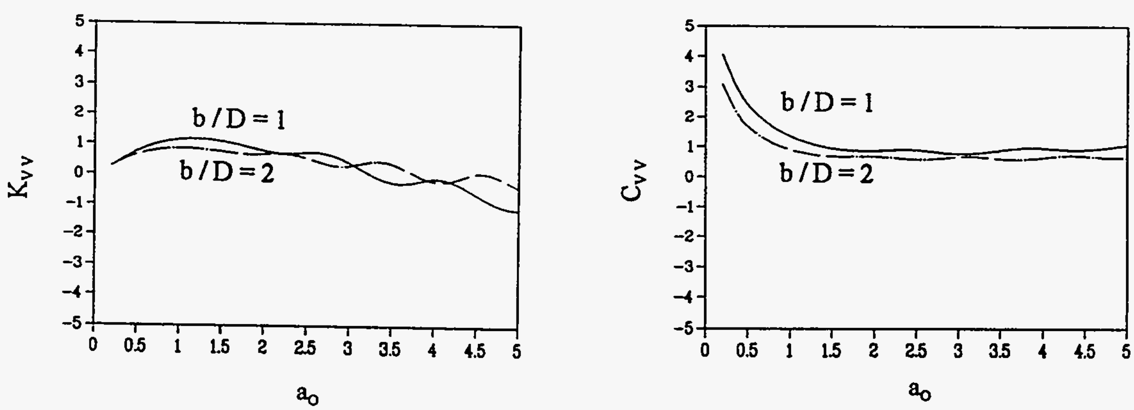

Figure 11. Horizontal Impedances. Case: H/b = ∞ Saturated Stratum ($\nu = \frac{1}{3}$; $\xi = 0.05$)

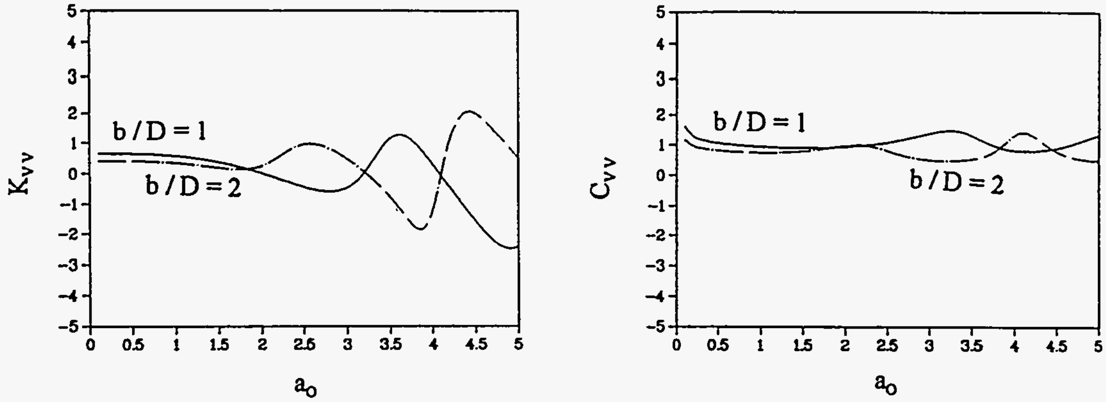

Figure 12. Horizontal Impedances. Case: H/b = 2 Dry Stratum ($\nu = \frac{1}{3}$; $\xi = 0.05$)

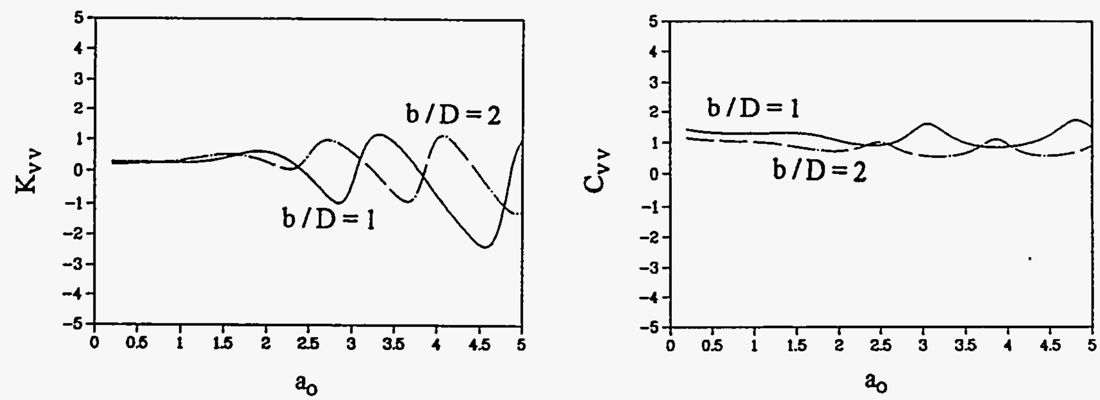

Figure 13. Horizontal Impedances. Case: H/b = 3 Dry Stratum ($\nu = \frac{1}{3}$; $\xi = 0.05$)

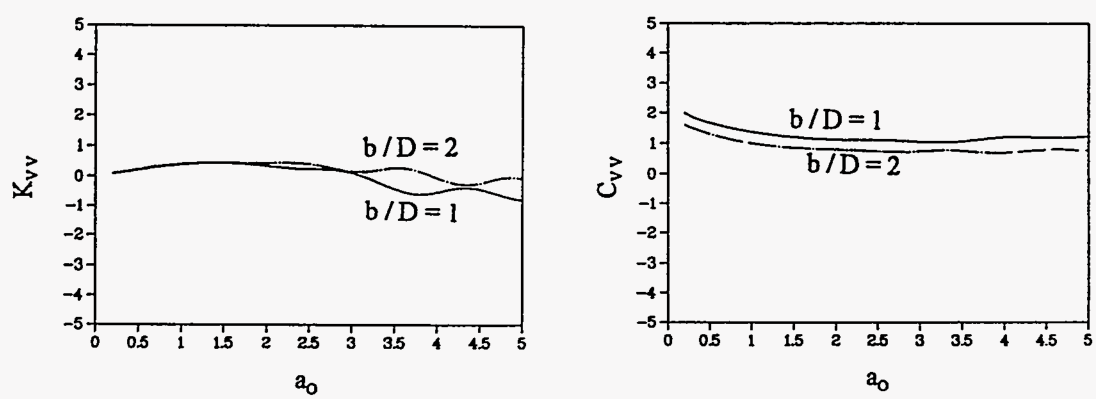

Figure 14. Horizontal Impedances. Case: H/b = ∞ Dry Stratum ($\nu = \frac{1}{3}$; $\xi = 0.05$)